Magnetotunneling Spectroscopy of Dilute Ga(AsN) Quantum Wells

Magnetotunneling Spectroscopy of Dilute Ga(AsN) Quantum Wells

J. Endicott, A. Patanè,* J. Ibáñez, L. Eaves, and M. Bissiri
School of Physics and Astronomy, University of Nottingham, Nottingham NG7 2RD, United Kingdom

M. Hopkinson, R. Airey, and G. Hill
Department of Electronic and Electrical Engineering, University of Sheffield, S3 3JD Sheffield, United Kingdom
(Received 7 May 2003; published 16 September 2003)

We use magnetotunneling spectroscopy to explore the admixing of the extended GaAs conduction band states with the localized N-impurity states in dilute $GaAs_{1-y}N_y$ quantum wells. In our resonant tunneling diodes, electrons can tunnel into the N-induced E_- and E_+ subbands in a $GaAs_{1-y}N_y$ quantum well layer, leading to resonant peaks in the current-voltage characteristics. By varying the magnetic field applied perpendicular to the current direction, we can tune an electron to tunnel into a given k state of the well; since the applied voltage tunes the energy, we can map out the form of the energy-momentum dispersion curves of E_- and E_+. The data reveal that for a small N content ($\sim 0.1\%$) the E_- and E_+ subbands are highly nonparabolic and that the heavy effective mass E_+ states have a significant Γ-conduction band character even at $k = 0$.

DOI: 10.1103/PhysRevLett.91.126802 PACS numbers: 73.40.Gk, 71.20.Nr

The incorporation of low concentrations of N ($y =$ 0–5%) in GaAs leads to a number of unusual physical properties [1–3]. In the ultradilute regime ($y < 0.01\%$), N introduces a single-impurity level at an energy of $\sim$0.2 eV above the conduction band minimum of GaAs [4]. A further increase of N causes a large band-gap bowing with a band-gap reduction of about 0.1 eV per atomic percent of N content [1–3,5,6]. This has raised the interesting possibility of using N-containing alloys grown in GaAs substrates for long-wavelength optoelectronic applications [7]. At present, research on $GaAs_{1-y}N_y$ represents one of the most active topics in semiconductor physics. However, despite years of extensive studies, there is not yet direct experimental evidence that the conduction band of $GaAs_{1-y}N_y$ has the hybridized character and highly nonparabolic energy–wave-vector dispersion that have been predicted by theory [5,6,8–11]. According to band anticrossing models, the interaction of the extended Γ-conduction band states of GaAs with the localized N energy level causes a splitting of the conduction band into two nonparabolic subbands E_- and E_+, as well as to additional states. The coexistence of different local environments in the alloy also complicates the electronic properties of $GaAs_{1-y}N_y$: Single N impurities form perturbed delocalized states in the host lattice whereas N aggregates, such as impurity N-N pairs and higher-order clusters, form strongly localized states; these two different types of states can admix to form a so-called ''amalgamated'' conduction band, thus leading to a duality of bandlike and localization behaviors [3,8,9].

In this Letter, we explore the electronic states of GaN_yAs_{1-y} quantum well (QW) layers using magnetotunneling spectroscopy (MTS). The MTS technique has been previously used to study the electronic properties of different semiconductor heterostructures [12–14] including valence band QWs [12] and quantum dots [14]. Here we show that the MTS can provide us with a powerful means of exploring the admixing of the extended conduction band states of GaAs with the localized N-impurity states. In our resonant tunneling diodes (RTDs), electrons can tunnel into the N-induced E_- and E_+ subbands in a GaN_yAs_{1-y} QW layer, thus leading to resonant peaks in the current-voltage characteristics, $I(V)$. Varying a magnetic field applied perpendicular to the current direction allows us to tune an electron to tunnel into a given k state of the well; the voltage tunes the energy so that we can map out the energy–wave-vector dispersion $\varepsilon(k)$ curves of the E_- and E_+ subbands. The data reveal that, for a small N content ($\sim 0.1\%$), the E_- and E_+ subbands are highly nonparabolic and that the heavy effective mass E_+ states have a significant Γ-conduction band character even at $k = 0$.

In this study, we used a series of five *n-i-n* $GaAs/Al_{0.4}Ga_{0.6}As/GaAs_{1-y}N_y$ RTDs grown by molecular beam epitaxy (MBE) on (100)-oriented *n*-type (Si: 1×10^{18} cm^{-3}) GaAs substrates. In our samples, an 8 nm thick $GaAs_{1-y}N_y$ ($y = 0$, 0.08, 0.43, 0.93, and 1.55%) layer is embedded between two 6 nm thick $Al_{0.4}Ga_{0.6}As$ tunnel barriers; undoped GaAs spacer layers of width 50 nm separate the $Al_{0.4}Ga_{0.6}As$ barriers from *n*-doped GaAs layers in which the dopant concentration is increased from 2×10^{17} cm^{-3}, close to the barrier, to 2×10^{18} cm^{-3}. The samples were processed into mesas with diameters ranging between 25 and 400 μm, with a ring-shaped metallic top contact layer to provide optical access for $I(V)$ measurements under illumination with above-band gap laser light (633 nm).

The inset of Fig. 1 shows schematically the conduction band profile of our RTDs. At zero bias, equilibrium is established by electrons diffusing from the doped GaAs layers into the N-induced localized states in the

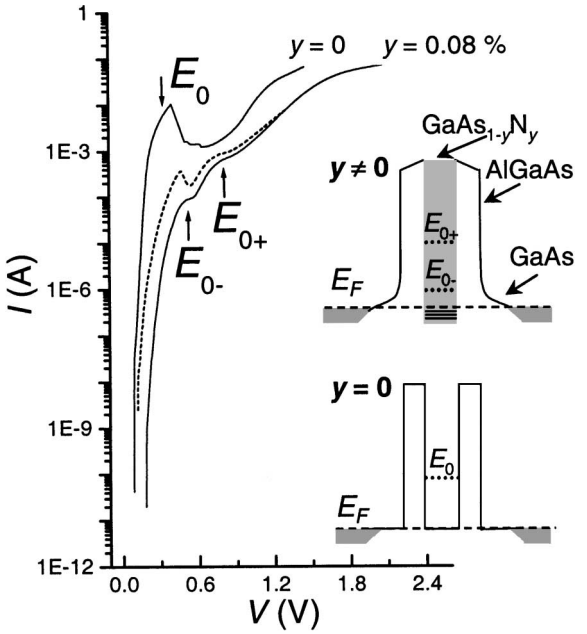

FIG. 1. $I(V)$ curves at $T = 4.2$ K incorporating $GaAs_{1-y}N_y$ layers with $y = 0$ and 0.08%. The dashed line is the $I(V)$ under illumination for the sample with $y = 0.08\%$. The insets sketch the conduction band profile at zero bias for a diode with and without N. When y is increased from 0 to 0.08%, the lowest quasibound state of the QW, E_0, splits into two bound states, E_{0-} and E_{0+}. In addition, N introduces localized states with energies below the GaAs conduction band edge.

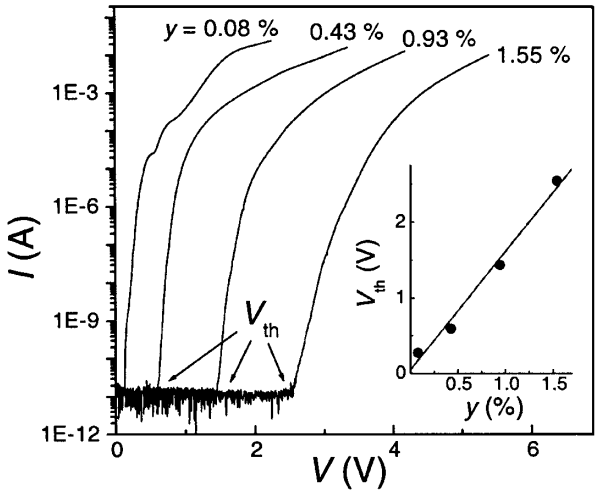

FIG. 2. $I(V)$ curves at $T = 4.2$ K for RTDs incorporating a $GaAs_{1-y}N_y$ layer with $y = 0.08\%$, 0.43, 0.93, and 1.55%. The inset shows the dependence of the threshold voltage V_{th} on y.

$GaAs_{1-y}N_y$ layer, e.g., N-cluster states and N-related defects with energies below the GaAs conduction band edge [15]. Negative charge in the well gives rise to two depletion layers in the regions beyond the $Al_{0.4}Ga_{0.6}As$ barriers and a corresponding band bending. When a voltage is applied, resonant tunneling through a particular subband state in the $GaAs_{1-y}N_y$ QW layer gives rise to a peak in $I(V)$, whenever this state is resonant with an adjacent filled state in the negatively biased electron emitter layer. As shown in Fig. 1, when y is increased from 0 to 0.08%, the resonance E_0 due to electrons tunneling through the lowest bound state of the QW splits into two main features, E_{0-} and E_{0+}. These can be seen more clearly in the $I(V)$ measured under illumination (see dashed line in Fig. 1). In contrast, as shown in Fig. 2, further increase of y smears out the resonances (weak features are revealed in the differential conductance, dI/dV, plot), quenches the current, and shifts to higher biases the threshold voltage, V_{th}, at which the current increases rapidly.

The monotonic shift of V_{th} to higher biases with increasing y is consistent with an increasing charge in the well due to formation of denser low-energy N states that act as traps of electrons. The negative charge in the well and the resulting bending of the conduction band become more pronounced with increasing y and tend to inhibit the current flow at low voltages. The smearing of the resonances at large y is likely to be due to an increasing disorder in the system. In the absence of disorder, both the energy and the in-plane momentum of the electron are conserved in the tunneling process; these are the conditions required to observe a peak in the $I(V)$ curve. At low y ($y = 0.08\%$), the disorder in the well is weak and tunneling of electrons through the QW subbands leads to the peaks E_{0-} and E_{0+} in $I(V)$. A further increase of y increases the probability of alloy fluctuations and formation of N clusters with strongly localized levels. The destruction of translational symmetry due to disorder tends to break the momentum conservation condition and smears out the resonances, as is observed even for $y = 0.08\%$. The resonances observed for this sample can be enhanced by optical excitation. This enhancement is probably due to the effect of screening of the disorder in the QW by the photogenerated holes and to the effect on the current of hole recombination with majority electrons tunneling in the N-related states [16].

A magnetic field, B, applied parallel to the QW plane (X, Y) is used to probe in detail the $I(V)$ curves. For $y > 0.08\%$, the $I(V)$ are almost unaffected by the magnetic field up to the available field of 12 T, thus suggesting that the current is due to tunneling of electrons through localized N-related states, as was also observed for similar RTDs with $y \sim 2\%$ [17]. In contrast, resonances E_{0-} and E_{0+} in the $I(V)$ plot of the RTD with $y = 0.08$ are strongly affected by B. Figures 3(a) and 3(b) show the B dependence of the $I(V)$ plots under illumination for $y = 0.08\%$. An identical B dependence of the resonant peaks in the $I(V)$ curves was also measured in dark conditions. The data show a shift to higher bias of E_{0-} and E_{0+} and a general increase of current with increasing B. However, the relative weight of E_{0-} and E_{0+} changes significantly with B. The B dependence of the amplitude of the E_{0-} and E_{0+} peaks in $I(V)$ has the characteristic form of a quantum mechanical admixing effect, i.e., with increasing B, the E_{0-} feature tends to become weaker and

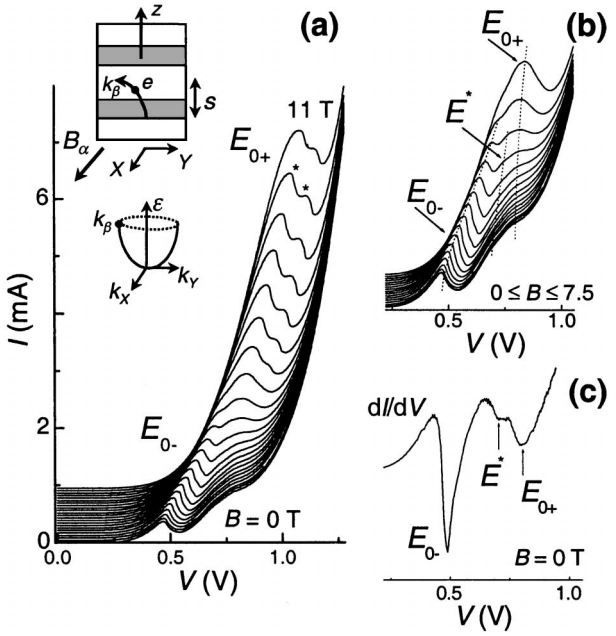

FIG. 3. (a) $I(V)$ curves under illumination at $T = 4.2$ K and various B for a RTD with $y = 0.08\%$. B is increased from 1 to 11 T by steps of 0.5 T. For clarity, the curves are displaced along the vertical axis. The double step decrease of $I(V)$ marked by asterisks on one of the high-field curves arises from the instability in the current due to the strong negative differential conductance. The left inset is a sketch of the magnetotunneling experiment. (b) $I(V)$ curves with B in the range 0 to 7.5 T. Dotted lines are guides to the eye and show resonances E_{0-}, E_{0+}, and E^*. (c) Differential conductance, dI/dV, plot for $B = 0$ T.

disappear, whereas the E_{0+} peak increases significantly in amplitude. Also, the $I(V)$ curves show a further weak feature (E^*), which shifts to higher bias with increasing B and disappears for $B > 6$ T. This feature is more clearly revealed in the differential conductance plot shown in Fig. 3(c). By carrying out a series of measurements for different orientations of B in the (100) growth plane, we find that both the intensity and bias position of the resonances are isotropic.

We can understand the B dependence of the resonances in terms of the effect of B on an electron tunneling into the states of the $GaAs_{1-y}N_y$ QW. Let α, β, and Z indicate, respectively, the direction of B, the direction normal to B in the growth plane, and the normal to the tunnel barrier, respectively. Because of the action of the Lorentz force, when an electron tunnels from the emitter into the well, it acquires an additional in-plane momentum given by $k_\beta = eBs/\hbar$, where s is the tunneling distance from the emitter to the QW. The structure of our device indicates that s is approximately equal to 30 nm: The sum of the barrier width plus the half-width of the $GaAs_{1-y}N_y$ well is 10 nm, and we also need to take into account the spread of the electron wave function in the emitter region adjacent to the $Al_{0.4}Ga_{0.6}As$ barrier (~ 20 nm). Varying B allows us to tune an electron to tunnel into a given k_β state of the well; the voltage tunes the energy so that by measuring the voltage position of the peaks in $I(V)$ as a function of B, we can map out the energy–wave-vector dispersion curve $\varepsilon(k_\beta)$ of the $GaAs_{1-y}N_y$ QW layer.

Figure 4(a) shows the B and k dependence of the voltage position of the current features E_{0-}, E_{0+}, and E^*. The $V(k)$ plots for E_{0-} and E_{0+} resemble the dispersion curves $\varepsilon(k)$ of the E_- and E_+ subbands calculated by using a two-band anticrossing model of bulk $GaAs_{1-y}N_y$ [see Fig. 4(b)] [5]. This suggests that E_{0-} and E_{0+} arise, respectively, from electron tunneling into the N-induced E_- and E_+ subbands of the $GaAs_{1-y}N_y$ QW layer. However, as shown in Fig. 4(c), the QW confinement has the effect of modifying the detailed form of the $\varepsilon(k)$ curves associated with E_- and E_+ [18]: The hybridization between the first QW subband states qw_0 and the N-impurity level occurs at k values smaller than those for bulk GaAs, as also observed experimentally, and leads to subbands E_{0-} and E_{0+} with smaller energy separation than for the bulk case; the QW confinement effect also gives rise to additional subbands, E_{1-} and E_{1+}, arising from the hybridization of the higher energy QW subband states qw_1 with the N-impurity level. The latter effect may explain the presence of the E^* resonance and the form of its associated $\varepsilon(k)$ dispersion curve. We attribute the E^* resonance to electron tunneling into the E_{1-} states. As shown in Fig. 4(c), the energy minimum of the qw_1 subband is very close to the N level, which gives rise to

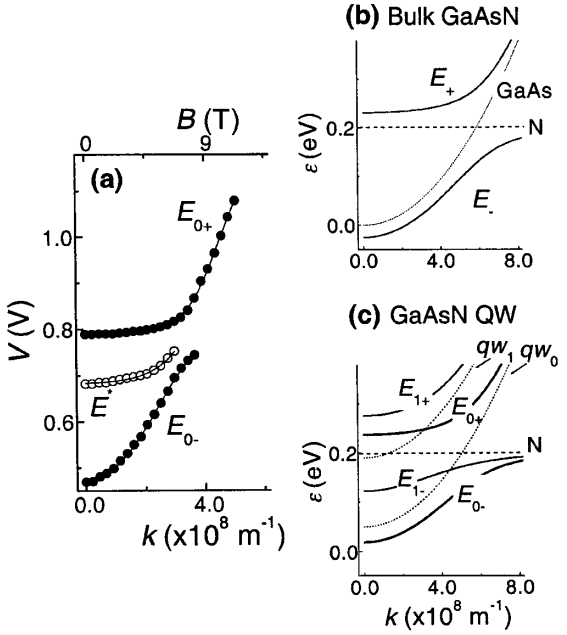

FIG. 4. (a) Voltage position of current peaks E_{0-}, E_{0+}, and E^* in $I(V)$ as a function of B (top axis) and of $k = esB/\hbar$ (bottom axis). (b) Energy–wave-vector dispersion curves for bulk $GaAs_{1-y}N_y$. (c) Energy–wave-vector dispersion curves for a $GaAs_{1-y}N_y$ QW (continuous lines) and for a GaAs QW (dotted lines). The energies are measured relative to the minimum of the GaAs conduction band and the N content is equal to 0.08%.

a weak E_{1-} energy dispersion as is observed for E^*. Since the voltage position of E_{0-}, E_{0+}, and E^* does not depend on the orientation of B in the QW plane, we deduce that the anisotropy in $\varepsilon(k_X, k_Y)$ for all subbands is negligible at small $k(\sim B)$ values.

A precise correlation between the measured value of V and ε is limited by the fact that the electrostatic leverage factor, f, the parameter that controls the scale of energy values [$f = e(dV/d\varepsilon)$] is not known precisely. However, if we assume a value of $f \sim 2$, as expected within a simple electrostatic model of our device, we find that the energy separation Δ between the E_- and E_+ subbands is smaller (~ 0.16 eV) than that predicted by theory for bulk $GaAs_{1-y}N_y$ (~ 0.25 eV). Also, the $V(k)$ curves show an anticrossing effect at a value of $k \sim 4 \times 10^8$ m^{-1} smaller than that predicted for bulk $GaAs_{1-y}N_y$ ($k \sim 6 \times 10^8$ m^{-1}) [18]. This suggests that the lowered dimensionality of the QW acts to modify the band structure of the $GaAs_{1-y}N_y$ layer with respect to the bulk case.

Finally, the B dependence of the amplitude of the E_{0-} and E_{0+} features in $I(V)$ reveals interesting details about the nature of the E_- and E_+ subbands. The magnitude of the tunnel current is proportional to the modulus squared of the tunneling matrix element between the in-plane components of the emitter and QW states. At $B = 0$, the conservation of the in-plane wave vector implies that the QW states into which an electron can tunnel must have at least a partial Γ-like character, since the states of the GaAs emitter are almost pure Γ states. Since E_{0+} is observed at $B = 0$, we infer that the very weakly dispersed E_+ states have a significant Γ-conduction character even at $k = 0$. The strong enhancement of the E_{0+} resonance at large B and the corresponding increase of the momentum-energy dispersion at large k ($k \sim B$) indicate that, with increasing k, the E_+ subband states become more localized in real space. In contrast, the disappearance of the E_{0-} resonance at large B indicates that the E_- subband states become strongly localized at large k values. The E^* feature in $I(V)$ has a similar dependence as E_{0-}, which confirms our assignment of this resonance to tunneling into states of the E_{1-} subband.

In conclusion, magnetotunneling spectroscopy can provide us with a powerful means of probing the N-induced states in a dilute $GaAs_{1-y}N_y$ QW. The data reveal that, for a small N content ($\sim 0.1\%$), the N-induced E_- and E_+ subbands have a very well-defined character and that the heavy effective mass E_+ states have a significant Γ-conduction band character even at $k = 0$. Our results suggest that the highly nonparabolic dispersion of E_- and E_+ could be tailored by the QW confinement and exploited to design novel band-structure engineered devices with negative differential velocity characteristics, similar to those occurring in semiconductor superlattices or Gunn diodes [19,20].

This work is supported by the Engineering and Physical Sciences Research Council (United Kingdom) and by the Spanish Ministry of Science and Technology under CICYT Project No. MAT 2001-1878.

*Author to whom correspondence may be addressed. Electronic address: Amalia.Patane@nottingham.ac.uk

[1] M. Kondow, K. Uomi, A. Niwa, T. Kitatani, S. Watahiki, and Y. Yazawa, Jpn. J. Appl. Phys. **35**, 1273 (1996), Pt. 1.
[2] M. Weyers, M. Sato, and H. Ando, Jpn. J. Appl. Phys. **31**, L853 (1992), Pt. 2.
[3] For a review article on dilute nitrides, see C. Skierbiszewski *et al.*, Phys. Rev. B **65**, 035207 (2001), and references therein.
[4] H. P. Hjalmarson, P. Vogl, D. J. Wolford, and J. D. Dow, Phys. Rev. Lett. **44**, 810 (1980).
[5] W. Shan, W. Walukiewicz, J. W. Ager, E. E. Haller, J. F. Geisz, D. J. Friedman, J. M. Olson, and S. R. Kurtz, Phys. Rev. Lett. **82**, 1221 (1999).
[6] A. Lindsay and E. P. O'Reilly, Solid State Commun. **112**, 443 (1999).
[7] M. Kondow and T. Kitatani, IEE Proc. Optoelectronics **150**, 9 (2003).
[8] P. R. C. Kent and A. Zunger, Phys. Rev. B **64**, 115208 (2001).
[9] P. R. C. Kent and A. Zunger, Appl. Phys. Lett. **79**, 2339 (2001).
[10] T. Mattila, Su-Huai Wei, and A. Zunger, Phys. Rev. B **60**, R11245 (1999).
[11] A. Lindsay and E. P. O'Reilly, Solid State Commun. **118**, 313 (2001).
[12] R. K. Hayden, D. K. Maude, L. Eaves, E. C. Valadares, M. Henini, F. W. Sheard, O. H. Hughes, J. C. Portal, and L. Cury, Phys. Rev. Lett. **66**, 1749 (1991).
[13] P. H. Beton, J. Wang, N. Mori, L. Eaves, P. C. Main, T. J. Foster, and M. Henini, Phys. Rev. Lett. **75**, 1996 (1995).
[14] E. E. Vdovin, A. Levin, A. Patanè, L. Eaves, P. C. Mian, Yu. N. Khanin, Yu. V. Dubrovskii, M. Henini, and G. Hill, Science **290**, 122 (2000).
[15] P. Krispin, S. G. Spruythe, J. S. Harris, and K. H. Ploog, Appl. Phys. Lett. **80**, 2120 (2002).
[16] J. Ibáñez, J. Endicott, A. Patanè, M. Bissiri, L. Eaves, M. Hopkinson, R. Airey, and G. Hill (unpublished).
[17] A. Neumann, A. Patanè, L. Eaves, A. E. Belyaev, D. Gollub, A. Forchel, and M. Kamp, IEE Proc. Optoelectronics **150**, 49 (2003).
[18] For bulk $GaAs_{1-y}N_y$, we calculate the energy–wave-vector dispersion curves of the E_- and E_+ subbands by using the relation $E_\pm(k) = \frac{1}{2}\{[E_M(k) + E_N] \pm \sqrt{[E_M(k) - E_N]^2 + 4yC_{MN}^2}\}$, where $E_M(k)$ is the energy–wave-vector dispersion curve of GaAs, E_N is the energy position of the N-related level ($E_N = 1.725$ eV at 4.2 K), and C_{MN} is the hybridization matrix element ($C_{MN} = 2.7$ eV). For the case of the $GaAs_{1-y}N_y/Al_{0.4}Ga_{0.6}As$ QW, we use the same relation but with $E_M(k)$ equal to the energy–wave-vector dispersion curve for each subband of the $GaAs/Al_{0.4}Ga_{0.6}As$ QW.
[19] L. Esaki and R. Tsu, IBM J. Res. Dev. **14**, 61 (1970).
[20] J. B. Gunn, Solid State Commun. **1**, 88 (1963).